Published in final edited form as:

Int J Pharm. 2021 January 25; 593: 120120. doi:10.1016/j.ijpharm.2020.120120.

The enhanced intestinal permeability of infant mice enables oral protein and macromolecular absorption without delivery technology

John P. Gleeson[1], **Katherine C. Fein**[1], **Namit Chaudhary**[1], **Rose Doerfler**[1], **Alexandra N. Newby**[1], **Kathryn A. Whitehead**[1,2,*]

[1]Department of Chemical Engineering, Carnegie Mellon University, Pittsburgh, PA 15213.

[2]Department of Biomedical Engineering, Carnegie Mellon University, Pittsburgh, PA 15213.

Abstract

Oral delivery of macromolecular drugs is the most patient-preferred route of administration because it is painless and convenient. Over the past 30 years, significant attention has been paid to oral protein delivery in adults. Unfortunately, there is an outstanding need for similar efforts in infants, a patient population with distinct intestinal physiology and treatment needs. Here, we assess the intestinal permeability of neonatal and infant mice to determine the feasibility of orally delivering peptide and protein drugs without permeation enhancers or other assistance. Using the non-everted gut sac model, we found that macromolecular permeability depended on molecular size, mouse age, and intestinal tissue type using model dextrans. For example, the apparent permeability of 70 kDa FITC-Dextran (FD70) in infant small intestinal tissue was 2–5-fold higher than in adult tissue. As mice aged, the expression of barrier-forming and pore-forming tight junction proteins increased and decreased, respectively. The *in vivo* oral absorption of 4 kDa FITC-Dextran (FD4) and FD70 was significantly higher in younger mice, and there was a fourfold increase in oral absorption of the 80 kDa protein lactoferrin compared to adults. Oral gavage of insulin (5 IU/kg) reduced blood glucose levels in infants by >20% at 2 and 3 hours but had no effect in adults. Oral insulin had 35% and <1% of the pharmacodynamic effect of a 1 IU/kg subcutaneous dose in infants and adults, as measured by area above the curve. These data indicate that the uniquely leaky nature of the infantile intestine may support the oral delivery of biologics without the need for traditional oral delivery technology.

Keywords

oral drug delivery; protein delivery; pediatric therapy; tight junctions; intestinal permeability

1 Introduction

Oral drug delivery is attractive to patients due to its ease, and there has been great success in formulating small molecule drugs [1]. Unfortunately, most peptide and protein drugs have poor oral bioavailability due to their large size and physicochemical characteristics and must

*Corresponding author: Kathryn A. Whitehead, kawhite@cmu.edu.

be administered parenterally [2]. Because injections are often inconvenient, painful, and cause noncompliance, significant research has focused on the development of oral formulations for biologic drugs in adults [3]. Oral delivery solutions for infants have received significantly less attention [4], even though many infants receive injections of biopharmaceuticals (e.g. vaccines, anti-TNFα) [5]. Thus, we were motivated here to evaluate macromolecular delivery in infant populations.

To be delivered orally, macromolecules must survive the harsh acidic and proteolytic environment of the stomach and permeate across the intestinal mucus and epithelium to reach systemic circulation [6]. In adults, the key challenge preventing oral peptide and protein delivery is low intestinal permeability. The barrier function of the intestine is governed by intercellular protein complexes called tight junctions that restrict the paracellular passage of molecules larger than ~600 Da [7]. In adults, this has necessitated the incorporation of permeation enhancers into oral biologic formulations to transiently dilate the paracellular space [8–10]. Interestingly, infantile mouse intestinal tissue has markedly lower expression of tight junctional proteins compared to adult tissue [11]. So, while oral peptide delivery in adults requires permeation enhancers, pediatric oral biologic delivery may be possible without them.

In this study, we sought to fill a critical knowledge gap in the oral delivery literature by characterizing the permeability of the infant gut in mice. We hypothesized that the undeveloped nature of the infant gastrointestinal tract may facilitate sufficient oral absorption of macromolecular drugs to elicit a therapeutic effect without the use of enhancers or devices. Here, we assess the permeability of model macromolecules using intestinal tissue from mice of varied age and show that the higher permeability of the infant intestine enables the systemic absorption of protein drugs. These data suggest that murine infants are more amenable to oral delivery than adults and that it may be possible to develop oral biologic formulations for infants without enhancers, devices, or delivery technology.

2 Materials and Methods

2.1 Materials

Bovine pancreas insulin, FITC-Dextrans, Lactoferrin, and Krebs-Henseleit buffer were purchased from Sigma-Aldrich. Aimstrip Plus blood glucose strips, blood glucose monitor, and suture thread were obtained from VWR. Lactoferrin ELISA kits were purchased from Abcam. qRT-PCR reagents and kits were purchased from LifeTechnologies.

2.2 Non-everted gut sac to measure apparent permeability coefficient of fluorescent dextrans

All mouse experiments were approved by institutional animal care and use committee at Carnegie Mellon University under protocol no. PROTO201600017 and performed in accordance with all institutional, local, and federal regulations. C57BL/6 mice were housed in a pathogen-free environment with controlled conditions of humidity and temperature under a 12:12 h light/dark cycle with access to laboratory chow and filtered water ad libitum. Two-, four-, and twelve-week-old mice were euthanized by carbon dioxide, and a

midline laparotomy was performed. The stomach, proximal small intestine, distal small intestine, and colon were excised and placed directly in cold Krebs-Henseleit buffer. The stomachs were flushed with cold Krebs-Henseliet buffer and ligated at the lower esophageal sphincter and above the pyloric sphincter. The intestinal pieces were flushed with cold Krebs-Henseleit buffer, and 2–4 cm segments were ligated with 0.08 mm suture thread. The gut sacs were then injected using 31G needles with FITC-labeled dextrans (1 mg/ml) of four molecular weights: 4 kDa (FD4), 10 kDa (FD10), 70 kDa (FD70), and 150 kDa (FD150) [12]. The gut sacs were then placed in 20 ml of Krebs-Henseleit buffer gassed with carbogen (95% O_2, 5% CO_2), and samples were taken from the buffer every 30 min for 2 hours. The FD signal intensity was measured using a TECAN fluorescent plate reader at excitation/emission wavelengths of 490 nm/525 nm. After 2 hours had elapsed, the gut sacs were removed from the buffer, cut open, and the surface area was measured. The apparent permeability coefficient (P_{app}) was calculated according to the equation [8]:

$$P_{app} = \frac{dQ}{dt} x \frac{1}{A \cdot C_0}$$

where dQ/dt is the transport rate/slope of the line, A is the surface area, and C_0 is the starting concentration of flux marker injected. Permeability experiments were carried out with a minimum of five independent replicates.

2.3 Analysis of tight junction gene expression by qRT-PCR

Tissue samples (1 cm) were taken adjacent to gut sac prepared tissue. Tissues were placed into Trizol reagent (0.5 ml) and homogenized using the BeadBug microtube homogenizer. Chloroform (0.1 ml) was added, and the resultant mixture was centrifuged at 12,000 rpm for 15 min. The aqueous layer was removed and mixed with an equal amount of 100% ethanol, and the RNA was extracted with RNeasy mini kit (Qiagen). cDNA was generated from 2 μg of RNA using High-Capacity cDNA Reverse Transcription Kit (Applied Biosystems). Quantitative real-time polymerase chain reaction (qRT-PCR) was performed using SYBR Select Master Mix (Applied Biosystems) on a ViiA 7 Real-Time PCR system (Applied Biosystems). Primer sequences as follows:

Gene	Forward	Reverse
BACTIN	CACTGTCGAGTCGCGTCC	TCATCCATGGCGAACTGGTG
CLDN1	GCCATCTACGAGGGACTGTG	CCCCAGCAGGATGCCAATTA
CLDN2	GAAAGGACGGCTCCGTTTTC	CAGTGTCTCTGGCAAGCTGA
CLDN3	GTACAAGACGAGACGGCCAA	GGGCACCAACGGGTTATAGA
CLDN4	CCACTCTGTCCACATTGCCT	CTTTGCACAGTCCGGGTTTG
CLDN5	GTTAAGGCACGGGTAGCACT	TACTTCTGTGACACCGGCAC
CLDN7	CAAGGGCCCGCATACTTTCT	TGGTTCCAGACAAAAGCGGT
CLDN8	GGAATGCCAATCCATCACGC	CTCTTTTATCCCCAGGCCCC
CLDN12	CCCGATGGATGCTAGGAACT	GAGGCTTCAGGGAACCAGTC

CLDN13	CCCTGTCCTGGGTAACACAC	AGGGAGAGTGAAGAGCCCAT
CLDN15	GGTGGCTATCTCGTGGTACG	GCACTCCAGCCCAAGTAGAG
ZO1	CTCTTCAAAGGGAAAACCCGA	GTACTGTGAGGGCAACGGAG
ZO2	GCGCGAGATGCCGGT	ATCCTCTTTTGGAATCCTTCTGC
ZO3	GTGGGGGCTGATTGTTTCCA	TCTGCCACCTGGAATCTCAC
OCCL	TTTCCTTAGGCGACAGCGG	CCAAGATAAGCGAACCTGCC
JAMA	TCCCGAGAACGAGTCCATCA	GAACTTCCACTCCACTCGGG
ITLN1	TAATGAGAGAGCGGCCAGTG	TCCACCGATGCAGTGATGTT

2.4 Immunofluorescence imaging of tight junctional proteins

Tissues were harvested after oral gavage experiments, fixed in 4% paraformaldehyde (Electron Microscopy Sciences), washed with phosphate buffered saline, and incubated in 30% sucrose solution at 4°C. Tissue was embedded in OCT and cryosectioned with 10 μm sections. Samples were blocked in 10% BSA (VWR) with 0.5% Triton X-100 and incubated with primary antibodies overnight at 4°C. Primary antibodies were as follows: Claudin 2 mouse monoclonal (Thermo Fisher), Claudin 3 rabbit polyclonal (Thermo Fisher). Secondary antibodies were as follows: Goat anti-mouse Alexa Fluor 488, goat anti-rabbit Alexa Fluor 488, goat anti-rabbit Alexa Fluor 594. Nuclei were stained with DAPI (0.5 μg/ml; Life Technologies). Images were obtained with a Zeiss LSM 700 microscope using Zen 2012 software.

2.5 In vivo oral absorption studies - insulin

Twelve-week-old mice were fasted 12 h prior to procedure with free access to water. Two-week-old pups could not be fasted or separated from their mother prior to absorption studies. Animals were weighed and randomized into groups: oral insulin (5 IU/kg), subcutaneous insulin (1 IU/kg), or oral phosphate buffered saline. Mice were gavaged with soft plastic oral gavage needles (Instech Laboratories), sized 22G and 20G for two- and twelve-week-old mice, respectively. Blood glucose levels were measured at 0, 1, 2, 3, and 4 h for all groups by submandibular bleed, with additional measurements at 0.25 and 0.5 h for subcutaneous groups. Two-week-old pups were kept on a heat pad throughout the duration of the study. Oral gavage and subcutaneous groups had a minimum n of six and four, respectively. The area above the curve (AAC) of the blood glucose levels of insulin was calculated using trapezoidal rule between the curve of interest and 100. The AAC was normalized for the two insulin treated groups by subtracting the AAC of the PBS negative control group.

2.6 In vivo oral absorption studies – FD4 and Lactoferrin/FD70 co-delivery

Animals were treated as per Section 2.4, and animals were gavaged with either FD4 (200 mg/kg) or FD70 (200 mg/kg). Blood samples were taken at 1 and 3 h by submandibular bleed. The blood serum area under the curve (AUC) was calculated using the trapezoidal rule. Additionally, animals were gavaged with Lactoferrin (320 mg/kg), and blood samples were taken at 2 h by submandibular bleed. Blood sample time points were based on preliminary experiments in two-week-old pups (data not shown). The FD signal intensity was measured using a TECAN fluorescent plate reader at excitation/emission wavelengths

of 490 nm/525 nm. Lactoferrin was assessed by human lactoferrin ELISA (Abcam). Oral gavage experiments were carried out with a minimum of six replicates.

2.7 Statistical analyses

All data are represented as mean ± standard error of the mean (SEM). Statistical analysis was carried out using Prism-7 software (GraphPad) using Student's t-test, one-way ANOVA, and two-way ANOVA with Dunnett's and Bonferroni's post hoc tests respectively. A significant difference was defined as $P < 0.05$.

3 Results

3.1 Infant small intestinal tissue is permeable to macromolecules less than 150 kDa

The infantile intestinal barrier has been reported to decrease in paracellular permeability over the weeks and months after birth in mice. Patel et al. demonstrated that maturation of gut barrier function occurs between week 2 and 3 of postnatal life in mice [13]. This observation was based on the oral absorption of FITC-Dextran 4 kDa (FD4). To better understand the intestinal permeability of larger macromolecules as a function of age, we assessed the permeability of four FITC-Dextrans: 4 kDa, 10 kDa (FD10), 70 kDa (FD70), and 150 kDa (FD150) in the non-everted gut sac model in mice. The apparent permeability (P_{app}) of these FITC-Dextrans was determined over two hours across the proximal small intestine, distal small intestine, and colon from mice aged 2, 4, and 12 weeks old (Table 1). These ages represent the neonatal-infantile period (2 weeks), early childhood (4 weeks), and adulthood (12 weeks) [14]. The permeability of FITC-Dextrans decreased as a function of dextran size, mouse age, and intestinal tissue location. There was a significant difference between the P_{app} of FD4, FD10, and FD70 across 2- and 12-week-old small intestinal tissue but not colonic tissue (Fig 1). As there was no difference in permeation at 2 vs. 4 weeks old, further experiments excluded the 4-week-old group and used only 2- and 12-week-old animals. Given recent literature evidence that macromolecules can be absorbed via the gastric epithelium [15], we also assessed the contribution of gastric permeability to FD4 and FD70 transport. The P_{app} of FD4 was five-fold higher in 2-week-old stomach sacs compared to 12-week-old animals, although, there was no difference in permeation of FD70 between 2- and 12-week-old stomach sacs. These data indicate that while 2-week-old mice have higher permeability throughout the gastrointestinal tract compared to adults, the increased absorption of larger macromolecules (e.g. 70 kDa) is due to enhanced permeability of the small intestine and not the stomach or colon. Compared to the small intestine and colon, the stomach contributed the least to macromolecular absorption in both infant and adult mice.

3.2 Tight junction gene expression and protein localization changes with mouse age

Tight junctional proteins control the paracellular pathway between intestinal epithelial cells, and, therefore, molecular permeability [16, 17]. To understand why infant and adult mice differed in FITC-Dextran permeabilities, we next assessed the gene expression and protein localization of 15 tight junction proteins in three segments of the intestine. All gene expression values in the proximal small intestine, distal small intestine, and colon in infant and adult mouse tissue are reported in Table 2. A subset of these data are displayed in Fig 2. Tight junctional proteins responsible for barrier integrity were downregulated in infant

tissues compare to adult tissue including Zonula occludins 1 (ZO-1), occludin (OCLN), junctional adhesion molecule-A (JAMA), and Claudin 3 (CLDN3) (Fig 2). For these proteins, a decrease in gene expression is related to an increased intestinal permeability. Furthermore, we observed upregulation of pore-forming CLDN2, which is directly linked with increase intestinal permeability [18, 19]. We also noted an increase expression in CLDN5, which has a poorly defined role in intestinal barrier integrity [20]. It has been reported that CLDN5 is upregulated during intestinal epithelial differentiation, which is increased in the developing intestine of infants [21]. The gene expression profiles of tight junction proteins are in line with previous reports [11] and explain the increased paracellular permeability observed in Fig 1.

We also stained intestinal sections for F-actin, which composes the cytoskeleton, and the tight junction proteins Claudin 2 and 3 (Fig 3). F-actin staining (left panels) showed that intestinal villus height, which corresponds to intestinal maturity, differed significantly between infant (254.7 ± 10.7 μm) and adult (427.7 ± 11.9 μm) tissue. Claudin 3 (middle panels), which is barrier-forming, was more abundant in adult tissue compared to infant tissue. It was localized in the mid-villus and tip regions in adult tissue and exclusively in crypts in infantile tissue. Intestinal stem cells are found in the crypts and move up the crypt-villus axis as they differentiate into enterocytes, and crypts are more abundant, larger, and active in infants [22]. The Claudin 3 localization is likely because of tissue maturation and indicates the decreased barrier function in infant tissue. Compared to Claudin 3, Claudin 2 protein expression (right panels) was lower in all mice and visible only under 40x magnification. In adult tissue, Claudin 2 was localized at the bicellular junction as expected [19, 23]. In contrast, it was localized intracellularly within some of the infant villi, indicating a stage of immaturity. Overall, the tight junction gene and protein expression data described here support the observation of increased permeability of 2-week-old mice compared to 12-week-old mice in the non-evert gut sac model.

3.3 Oral absorption of 4kDa and 70kDa fluorescent dextran is increased in infant mice

To confirm the data from the non-everted gut sac model in vivo, we next assessed the oral absorption of FD4 and FD70 in infant and adult mice. Mice were orally gavaged with 200 mg/kg of FD4, and blood serum levels were assessed over 3 hours. The FD4 blood serum levels were 0.55 μg/ml and 2.57 μg/ml for adults and infants, respectively (Fig 4A). This five-fold increase in oral absorption of FD4 observed *in vivo* was considerably higher than the two-fold increase in P_{app} in the *ex vivo* gut sacs.

Next, the same experiment was repeated with FD70 instead of FD4. After 3 hours, the FD70 blood serum levels were 0.12 μg/ml and 0.43 μg/ml for adults and infants, respectively (Fig 4B). This four-fold increase in FD70 oral absorption *in vivo* was again higher than the two-fold increase in P_{app} measured in the *ex vivo* gut sacs. Overall, oral absorption (as calculated from areas under the curve) was significantly higher in infants than adults for both size molecules (Fig 4C). These data show that infant mice absorb significant amounts of orally delivered macromolecules. Because these experiments were conducted with non-digestible dextrans, we next aimed to deliver functional proteins orally.

3.4 Infant intestinal permeability enables oral absorption of insulin and lactoferrin

In these experiments, delivery of functional insulin (5.8 kDa) was assessed by monitoring the blood glucose levels of recipient mice. Fasted adult and unfasted infant mice had resting blood glucose levels of 79 ± 9 mg/dL and 132 ± 8 mg/dL, respectively. Infant mice were not fasted for ethical reasons but were removed from the dam for the duration of the insulin studies (4 hours). Negative control mice of both ages were orally gavaged with PBS and maintained steady blood glucose concentrations for the duration of the 4-hour experiment. Positive control mice of both ages received subcutaneous (s.c.) injections of insulin (1 IU/kg) and, subsequently, experienced decreased blood glucose concentrations from 15 min through 3 hours post-injection (Fig 5A/B). Additionally, adults and infants were orally gavaged with 5 IU/kg insulin. Although blood glucose levels in adult mice did not change, infants experienced a significant decrease in blood glucose concentrations at 2 hours ($P > 0.001$) and 3 hours ($P > 0.05$). Area above the curve (AAC) analysis (Fig 5C) showed adults and infants responded similarly to subcutaneous injection. In contrast, infants experienced a significant response to oral insulin compared to adults (35% of s.c. vs. <1% of s.c.), suggesting that insulin survived transport across the intestinal epithelium into the systemic circulation.

Based on the oral absorption of 70 kDa FITC-dextran observed in infants (Fig 3), we next assessed the absorption of orally delivered model therapeutic protein, lactoferrin (80 kDa). In these experiments, we measured accumulation of lactoferrin in the systemic circulation by ELISA and quantified the gene expression of the lactoferrin transporter (Fig 6). Fasted adult and unfasted infant mice had similar basal blood concentrations of lactoferrin (49 ± 17 pg/ml and 47 ± 10 pg/ml, respectively). Two hours after animals received 320 mg/kg of human lactoferrin by oral gavage, blood lactoferrin concentrations were approximately 4-fold higher in infants versus adults (219 ± 17 pg/ml versus 48 ± 13 pg/ml, respectively) (Fig 6A). Because lactoferrin utilizes a transporter (intelectin 1; ITLN1) for absorption, we asked whether the increased absorption in infants was due to differences in ITLN1 expression. We found, however, that unlike tight junctional gene expression, there was no difference in ITLN1 mRNA expression in infant and adult small intestinal tissue (Fig 6B). This indicates that enhanced absorption in infant mice is not due to increased expression of the transporter and is more likely due exclusively to alterations in paracellular permeability. Together, these experiments with insulin and lactoferrin show that the infant intestinal physiology enables oral absorption of therapeutic macromolecules without the aid of a delivery system.

4 Discussion

There is a significant knowledge gap in the scientific literature regarding the oral delivery of macromolecular drugs in infants. Most of our knowledge of oral delivery is based on the well-studied adult intestinal tract and overlooks the underdeveloped nature of infants' intestines. Human neonates are born with developing gastrointestinal tracts that undergo "gut closure" within the first two days after birth [24, 25]. We suspect that oral macromolecular delivery in infants has not been previously pursued, in part, because the term "gut closure" is misleading. Gut closure specifically refers to a drop-off in the absorption of immunoglobulins (~150 kDa) in the neonatal intestine via FcRn-mediated

endocytosis [26]. Importantly, this does not speak to the permeability of macromolecules less than 150 kDa in size or to paracellular transport. Indeed, a handful of studies from the 1980s showed that the absorption of human alpha lactalbumin (~14 kDa) was 10–100 fold higher in human infants up to at least 3 months of age than in adults [27–29]. These data clearly demonstrate that oral macromolecular absorption is possible in human infants well after “gut closure” occurs. The window of increased permeability is likely a function of the size, shape, lipophilicity, and charge of the precise macromolecular drug in question.

To improve our understanding of oral delivery in infants and assess whether therapeutic macromolecular delivery may be possible, we conducted permeability experiments in an infant mouse model *ex vivo* and *in vivo*. Our data show that the paracellular pathway in infant mouse intestinal tissue is indeed more permeable than in adult intestinal tissue. Interestingly, the infant small intestinal tissue was significantly more permeable compared to adult tissue even with a macromolecule as large as 70 kDa Dextran (Fig 1). This suggests that the oral delivery of peptides, small proteins, and even small nucleic acids (e.g. GalNAc-siRNA) may be possible in infants based simply on the inherent leakiness of their intestinal tract [15]. Infants may not require the aid of intestinal permeation enhancers to improve the oral bioavailability of macromolecules, as in adults based on this animal data [30].

The higher paracellular permeability of infant intestinal tissue is likely due to complex expression patterns of tight junctional proteins. Holmes *et al.* observed decreased expression of barrier-forming claudins (e.g. claudin 3 and 5) and an increase in pore-forming claudins (e.g. claudin 2) in young mice [11]. Our data aligns with these observations, and we also noted significantly lower expression of ZO-1, ZO-3, occludin, and JAM-A in infant tissue (Fig 2, Table 2). Additionally, the protein abundance of claudin 2 was higher in infant tissue, although it was localized intracellularly (Fig 3). Claudin 2 mislocalization is commonly reported in diseases with increased permeability such as Crohn’s disease and necrotizing enterocolitis [19, 31]. Intestinal permeation enhancers have also been reported to affect the localization of tight junction proteins including claudin 2 and 5 [9, 32]. Therefore, the altered tight junctional protein expression and localization in infant tissue is most likely contributing to the higher basal permeability compared to adult tissue.

These data compelled us to assess the oral absorption of both a moderately sized peptide (insulin; 5.8 kDa) and a large protein (lactoferrin; 80 kDa) in infant and adult mice. Insulin is a clinically relevant therapeutic that is not absorbed across the adult intestine without the aid of a permeation enhancer [33, 34]. Lactoferrin was selected due its size and emerging evidence of clinical bioactivity [35, 36]. We also assessed the oral absorption of FITC-dextrans of similar size to insulin (4 kDa) and lactoferrin (70 kDa). The oral absorption of 4 kDa and 70 kDa FITC-dextran was significantly higher in infant mice (Fig 4), which is in agreement with data reported by Patel *et al.* using 4 kDa FITC-dextran [13]. Although oral delivery of insulin (5 IU/kg) did not affect blood glucose levels in adult mice, this modest dose significantly decreased blood glucose levels in infant mice (Fig 5). We anticipate that it would be possible to increase the oral insulin dose in diseased infants to produce therapeutically beneficial reductions in blood glucose levels. Similarly, the lactoferrin blood serum levels were significantly higher in infants compared to adults (Fig 6). Compared to FD70, which is a similar molecular weight, lactoferrin absorption was significantly lower.

Potential reasons for this decreased absorption may include denaturation/digestion of lactoferrin in the gut, a difference in aspect ratio of lactoferrin compared to dextran, differing surface charge and its effect on mucus penetration, or free lactoferrin binding to serum albumin in systemic circulation. Taken together, these data show that the device-free absorption of macromolecular drugs in infant animals is feasible. The literature on the oral absorption of human alpha lactalbumin (~14 kDa) in human infants [27–29], suggests that our results in mice may provide a basis to translate this work to human explants.

Stillhart *et al.* recently commented in their review that there are major gaps in knowledge related to pediatric oral drug absorption [37], specifically highlighting intestinal permeability, intestinal transporter expression, and the lack of pharmacokinetic data. This manuscript advances our fundamental understanding of the oral absorption of macromolecular drugs in infant models. Although data generated from rodent models do not always correlate with human drug absorption, we hope that the results presented here will spark interest in pediatric-specific oral medicines [4]. Encouragingly, the field has recently developed *in vitro* models that better reflect infant intestinal physiology, including IPEC-J2 cells and stem cell-derived intestinal organoids [38, 39]. Researchers are also engineering innovative patient-centric oral delivery systems for infants to overcome swallowing difficulties [40, 41]. These improvements in models and delivery systems will hopefully facilitate the translation of pediatric-centric medicines for this often-overlooked population.

5 Conclusion

In this study, we tested the hypothesis that the undeveloped nature of the infant gastrointestinal tract may enable the oral absorption of macromolecular drugs without the assistance of delivery technology in a mouse model. Using the non-everted gut sac model, we determined that the permeability of FITC-Dextran macromolecules was a function of dextran size, mouse age, and intestinal tissue type. The decreased expression of barrier-forming and increased expression of pore-forming tight junctional proteins contributed to the increased paracellular permeability in infant tissues. We also showed that infant mice absorb orally administered macromolecules, including Dextrans and functional proteins, into their bloodstreams to a significantly greater degree than adults. These data indicate that the leaky nature of the infantile intestine may support the oral administration of biologics without the aid of permeation enhancers, devices, or other delivery assistance.

Acknowledgements

This study was supported by the NIH Director's New Innovator Award – NICDH *DP2-HD098860*. Graphical abstract was created with BioRender.com.

References

[1]. Anselmo AC, Gokarn Y, Mitragotri S, Non-invasive delivery strategies for biologics, Nature Reviews Drug Discovery, 18 (2018) 19. [PubMed: 30498202]

[2]. Aguirre T, Teijeiro-Osorio D, Rosa M, Coulter I, Alonso MJ, Brayden DJ, Current status of selected oral peptide technologies in advanced preclinical development and in clinical trails, Advanced Drug Delivery Reviews, 106 (2016) 223–241. [PubMed: 26921819]

[3]. Brown TD, Whitehead KA, Mitragotri S, Materials for oral delivery of proteins and peptides, Nature Reviews Materials, 5 (2020) 127–148.

[4]. Batchelor HK, Fotaki N, Klein S, Paediatric oral biopharmaceutics: key considerations and current challenges, Adv Drug Deliv Rev, 73 (2014) 102–126. [PubMed: 24189013]

[5]. Cameron FL, Wilson ML, Basheer N, Jamison A, McGrogan P, Bisset WM, Gillett PM, Russell RK, Wilson DC, Anti-TNF therapy for paediatric IBD: the Scottish national experience, Arch. Dis. Child, 100 (2015) 399. [PubMed: 25678594]

[6]. Gleeson JP, McCartney F, Striving Towards the Perfect In Vitro Oral Drug Absorption Model, Trends Pharmacol. Sci, 40 (2019) 720–724. [PubMed: 31422894]

[7]. Shen L, Weber CR, Raleigh DR, Yu D, Turner JR, Tight junction pore and leak pathways: A dynamic duo, Annu. Rev. Physiol, 73 (2011) 283–309. [PubMed: 20936941]

[8]. Gleeson JP, Frías JM, Ryan SM, Brayden DJ, Sodium caprate enables the blood pressure-lowering effect of Ile-Pro-Pro and Leu-Lys-Pro in spontaneously hypertensive rats by indirectly overcoming PepT1 inhibition, Eur J Pharm Biopharm, 128 (2018) 179–187. [PubMed: 29684535]

[9]. Krug SM, Amasheh M, Dittmann I, C. I., Fromm M, Amasheh S, Sodium caprate as an enhancer of macromolecule permeation across tricullular tight junctions of intestinal cells, Biomaterials, 34 (2013) 275–282. [PubMed: 23069717]

[10]. McCartney F, Rosa M, Brayden DJ, Evaluation of Sucrose Laurate as an Intestinal Permeation Enhancer for Macromolecules: Ex Vivo and In Vivo Studies, Pharmaceutics, 11 (2019).

[11]. Holmes JL, Van Itallie CM, Rasmussen JE, Anderson JM, Claudin profiling in the mouse during postnatal intestinal development and along the gastrointestinal tract reveals complex expression patterns, Gene Expression Patterns, 6 (2006) 581–588. [PubMed: 16458081]

[12]. Mateer SW, Cardona J, Marks E, Goggin BJ, Hua S, Keely S, Ex vivo intestinal sacs to assess mucosal permeability in models of gastrointestinal disease, Journal of visualized experiments : JoVE, (2016) e53250. [PubMed: 26891144]

[13]. Patel RM, Myers LS, Kurundkar AR, Maheshwari A, Nusrat A, Lin PW, Probiotic bacteria induce maturation of intestinal claudin 3 expression and barrier function, The American journal of pathology, 180 (2012) 626–635. [PubMed: 22155109]

[14]. Dutta S, Sengupta P, Men and mice: Relating their ages, Life Sci, 152 (2016) 244–248. [PubMed: 26596563]

[15]. Buckley ST, Bækdal TA, Vegge A, Maarbjerg SJ, Pyke C, Ahnfelt-Rønne J, Madsen KG, Schéele SG, Alanentalo T, Kirk RK, Pedersen BL, Skyggebjerg RB, Benie AJ, Strauss HM, Wahlund P-O, Bjerregaard S, Farkas E, Fekete C, Søndergaard FL, Borregaard J, Hartoft-Nielsen M-L, Knudsen LB, Transcellular stomach absorption of a derivatized glucagon-like peptide-1 receptor agonist, Science translational medicine, 10 (2018) eaar7047. [PubMed: 30429357]

[16]. Van Itallie CM, Anderson JM, Architecture of tight junctions and principles of molecular composition, Semin. Cell Dev. Biol, 0 (2014) 157–165.

[17]. Hayashi M, Tomita M, Mechanistic analysis for drug permeation through intestinal membrane, Drug metabolism and pharmacokinetics, 22 (2007) 67–77. [PubMed: 17495413]

[18]. Barmeyer C, Schulzke JD, Fromm M, Claudin-related intestinal diseases, Semin. Cell Dev. Biol, 42 (2015) 30–38. [PubMed: 25999319]

[19]. Luettig J, Rosenthal R, Barmeyer C, Schulzke JD, Claudin-2 as a mediator of leaky gut barrier during intestinal inflammation, Tissue barriers, 3 (2015) e977176–e977176. [PubMed: 25838982]

[20]. Zhu L, Han J, Li L, Wang Y, Li Y, Zhang S, Claudin Family Participates in the Pathogenesis of Inflammatory Bowel Diseases and Colitis-Associated Colorectal Cancer, Frontiers in immunology, 10 (2019).

[21]. Dahan S, Roda G, Pinn D, Roth-Walter F, Kamalu O, Martin AP, Mayer L, Epithelial: lamina propria lymphocyte interactions promote epithelial cell differentiation, Gastroenterology, 134 (2008) 192–203. [PubMed: 18045591]

[22]. Cummins AG, Catto-Smith AG, Cameron DJ, Couper RT, Davidson GP, Day AS, Hammond PD, Moore DJ, Thompson FM, Crypt fission peaks early during infancy and crypt hyperplasia

broadly peaks during infancy and childhood in the small intestine of humans, J Pediatr Gastroenterol Nutr, 47 (2008) 153–157. [PubMed: 18664866]

[23]. Suzuki T, Yoshinaga N, Tanabe S, Interleukin-6 (IL-6) Regulates Claudin-2 Expression and Tight Junction Permeability in Intestinal Epithelium, The Journal of Biological Chemistry, 286 (2011) 31263–31271. [PubMed: 21771795]

[24]. Hurley WL, Theil PK, Perspectives on immunoglobulins in colostrum and milk, Nutrients, 3 (2011) 442–474. [PubMed: 22254105]

[25]. Vukavic T, Timing of the gut closure, J Pediatr Gastroenterol Nutr, 3 (1984) 700–703. [PubMed: 6502370]

[26]. Jaramillo CAC, Belli S, Cascais A-C, Dudal S, Edelmann MR, Haak M, Brun M-E, Otteneder MB, Ullah M, Funk C, Schuler F, Simon S, Toward in vitro-to-in vivo translation of monoclonal antibody pharmacokinetics: Application of a neonatal Fc receptor-mediated transcytosis assay to understand the interplaying clearance mechanisms, mAbs, 9 (2017) 781–791. [PubMed: 28440708]

[27]. Axelsson I, Jakobsson I, Lindberg T, Polberger S, Benediktsson B, Räihä N, Macromolecular absorption in preterm and term infants, Acta paediatrica Scandinavica, 78 (1989) 532–537. [PubMed: 2782068]

[28]. Jakobsson I, Lindberg T, Lothe L, Axelsson I, Benediktsson B, Human alpha-lactalbumin as a marker of macromolecular absorption, Gut, 27 (1986) 1029–1034. [PubMed: 3758816]

[29]. Lothe L, Lindberg T, Jakobsson I, Macromolecular absorption in infants with infantile colic, Acta paediatrica Scandinavica, 79 (1990) 417–421. [PubMed: 2349878]

[30]. Maher S, Mrsny RJ, Brayden DJ, Intestinal permeation enhancers for oral peptide delivery, Adv Drug Deliv Rev, 106 (2016) 277–319. [PubMed: 27320643]

[31]. Ares G, Buonpane C, Sincavage J, Yuan C, Wood DR, Hunter CJ, Caveolin 1 is Associated with Upregulated Claudin 2 in Necrotizing Enterocolitis, Scientific Reports, 9 (2019) 4982. [PubMed: 30899070]

[32]. Gleeson JP, Diet, food components and the intestinal barrier, Nutrition Bulletin, 42 (2017) 123–131.

[33]. Gedawy A, Martinez J, Al-Salami H, Dass CR, Oral insulin delivery: existing barriers and current counter-strategies, The Journal of pharmacy and pharmacology, 70 (2018) 197–213. [PubMed: 29193053]

[34]. Lamson NG, Berger A, Fein KC, Whitehead KA, Anionic nanoparticles enable the oral delivery of proteins by enhancing intestinal permeability, Nature Biomedical Engineering, (2019).

[35]. Giansanti F, Panella G, Leboffe L, Antonini G, Lactoferrin from Milk: Nutraceutical and Pharmacological Properties, Pharmaceuticals, 9 (2016).

[36]. Bruni N, Capucchio MT, Biasibetti E, Pessione E, Cirrincione S, Giraudo L, Corona A, Dosio F, Antimicrobial Activity of Lactoferrin-Related Peptides and Applications in Human and Veterinary Medicine, Molecules (Basel, Switzerland), 21 (2016).

[37]. Stillhart C, Vučićević K, Augustijns P, Basit AW, Batchelor H, Flanagan TR, Gesquiere I, Greupink R, Keszthelyi D, Koskinen M, Madla CM, Matthys C, Miljuš G, Mooij MG, Parrott N, Ungell A-L, de Wildt SN, Orlu M, Klein S, Müllertz A, Impact of gastrointestinal physiology on drug absorption in special populations—An UNGAP review, European Journal of Pharmaceutical Sciences, 147 (2020) 105280. [PubMed: 32109493]

[38]. Zakrzewski SS, Richter JF, Krug SM, Jebautzke B, Lee I-FM, Rieger J, Sachtleben M, Bondzio A, Schulzke JD, Fromm M, Günzel D, Improved cell line IPEC-J2, characterized as a model for porcine jejunal epithelium, PloS one, 8 (2013) e79643–e79643. [PubMed: 24260272]

[39]. Gleeson JP, Estrada HQ, Yamashita M, Svendsen CN, Targan SR, Barrett RJ, Development of Physiologically Responsive Human iPSC-Derived Intestinal Epithelium to Study Barrier Dysfunction in IBD, Int J Mol Sci, 21 (2020).

[40]. Lopez FL, Ernest TB, Tuleu C, Gul MO, Formulation approaches to pediatric oral drug delivery: benefits and limitations of current platforms, Expert opinion on drug delivery, 12 (2015) 1727–1740. [PubMed: 26165848]

[41]. Maier T, Bonner O, Peirce P, Slater NKH, Beardsall K, Drug and nutrient administration on the NICU – is delivery during breastfeeding an alternative to oral syringes?, Journal of Neonatal Nursing, (2019).

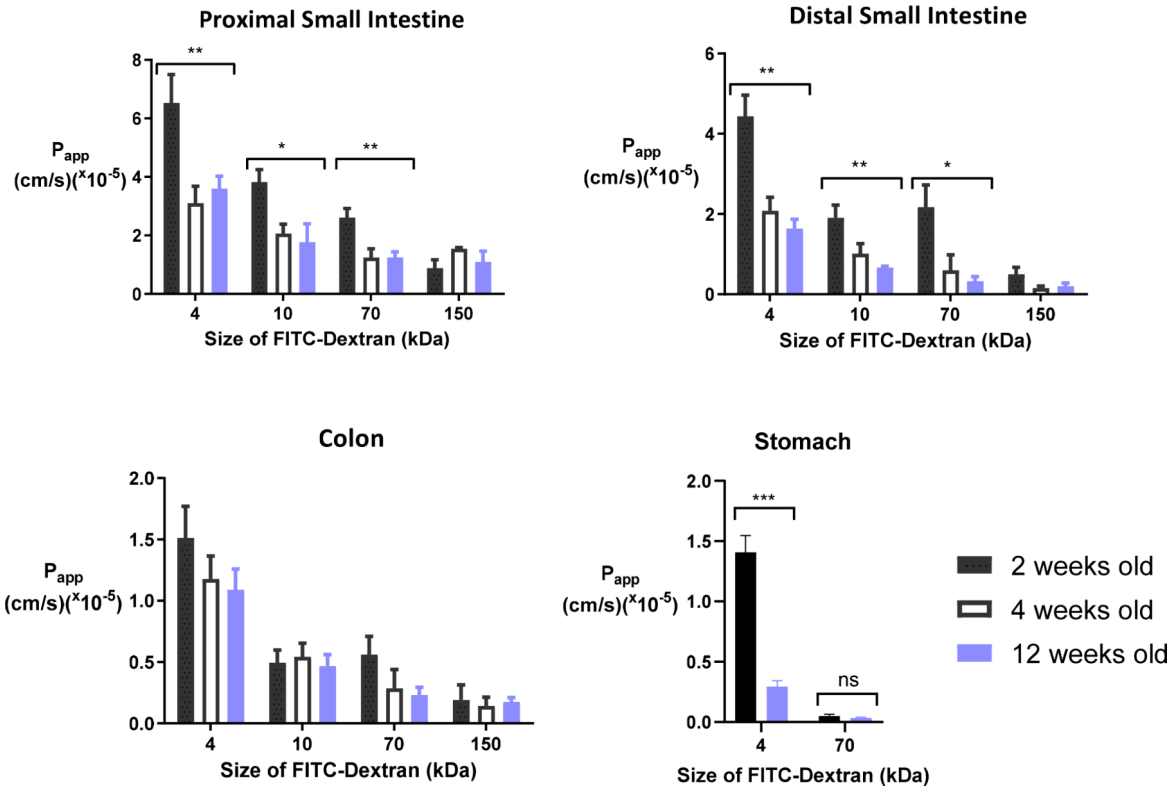

Fig. 1. Intestinal permeability of macromolecules is a function of molecular size, mouse age, and tissue type.

In these experiments, FITC-dextrans between 4 and 150 kDa were introduced into non-evert stomach or gut sacs from 2 week old (black), 4 week old (white) and 12 week old (blue) mice. Apparent permeability (P_{app}) in the intestine decreased with age, the size of the dextran, and the tissue's distance from the stomach. P_{app} values represent the mean ± SEM (n = 5). One-way ANOVA with Dunnett's multiple comparison test; * $P < 0.05$, ** $P < 0.01$, *** $P < 0.001$, compared to respective size marker in 12 week old mice.

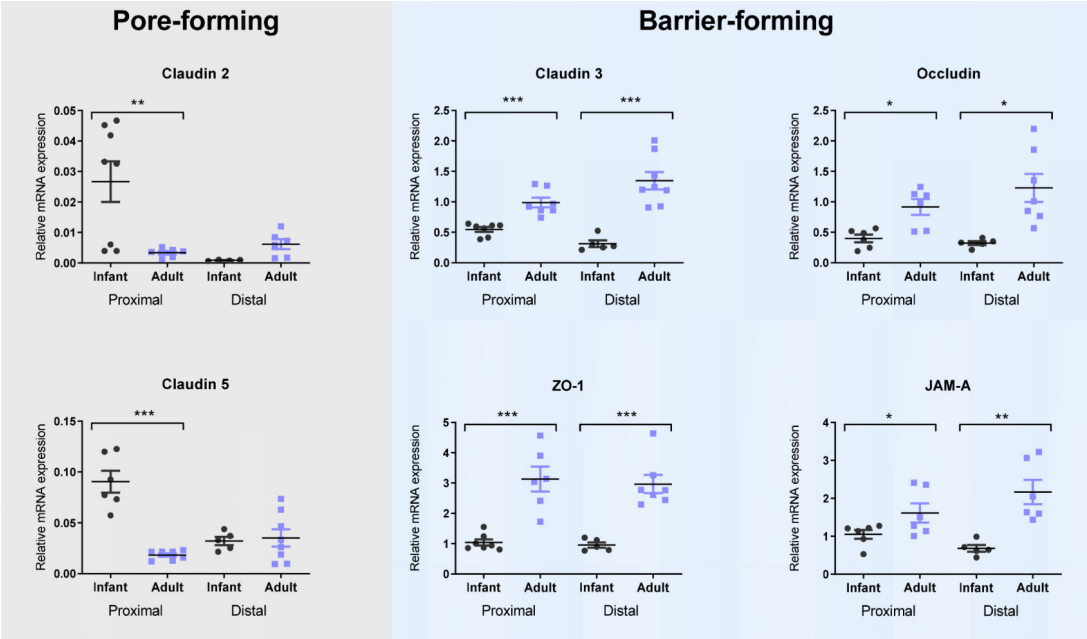

Fig. 2. –. Tight junction gene expression in the small intestine differed in infant mice and adults. Gene expression was measured using qRT-PCR on intestinal tissue from 2 week old (black) and 12 week old (blue) mice. Relative mRNA expression of the barrier-forming genes Claudin 3, Occludin, ZO-1, and JAM-A was lower in infantile tissue. Expression of the pore-forming genes Claudins 2 and 5 was higher in infantile tissue only in the proximal small intestine. Relative mRNA expression is expressed as percentage of β actin mean ± SEM (n = 6). One-way ANOVA with Tukey's multiple comparison test; * $P < 0.05$, ** $P < 0.01$, *** $P < 0.001$.

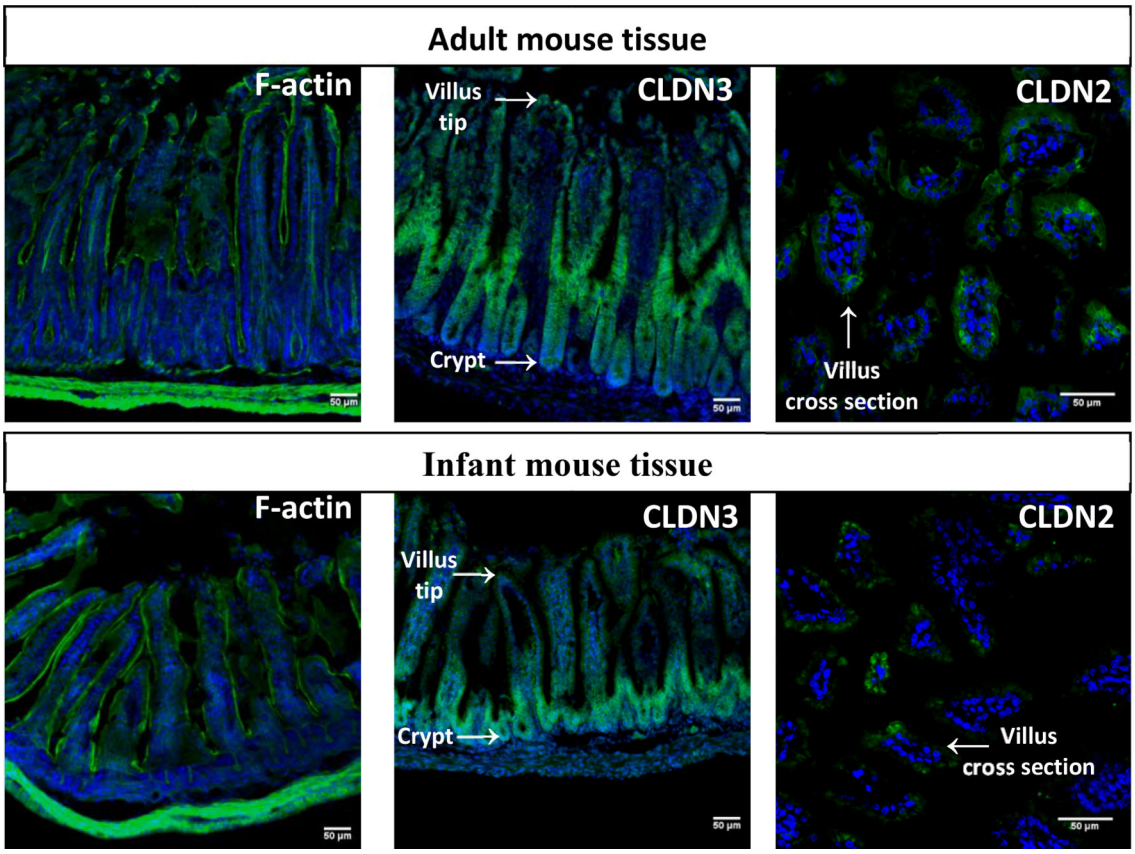

Fig. 3. –. Infant and adult intestinal mouse tissue differ in morphology and tight junction localization.

In each representative immunofluorescence image, nuclei are stained with DAPI (blue) and the protein of interest appears in green. Cytoskeleton (F-actin) staining showed taller, more mature villi in adult tissue. While the barrier-forming Claudin 3 (CLDN3) appears throughout adult villi, it is localized exclusively to the crypts in infant tissue. Cross sections of villi show localization of Claudin 2 (CLDN2) localized differently in adult tissue (towards cellular junctions) compared to infant tissue (intracellularly).

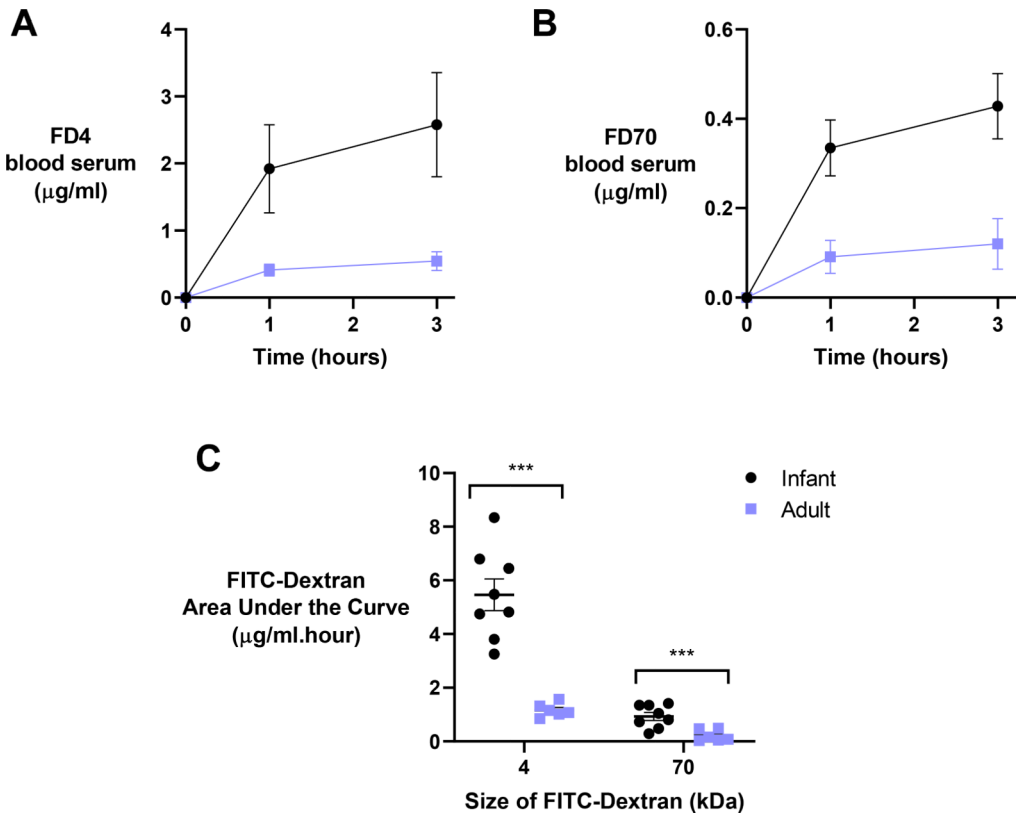

Fig. 4. –. Oral absorption of macromolecular dextrans is significantly higher in infant mice compared to adults.

In these experiments, A) 4 kDa and B) 70 kDa FITC-dextrans were orally administered to 2-week-old (infant; black) and 12-week-old (adult; blue) mice at a dose of 200 mg/kg. C) Resultant areas under the curve for both FD4 and FD70 decreased significantly in older animals over 3 hours. Values represent the mean ± SEM (n = 6). Student's unpaired *t* test: *** $P < 0.001$ compared to adult mice.

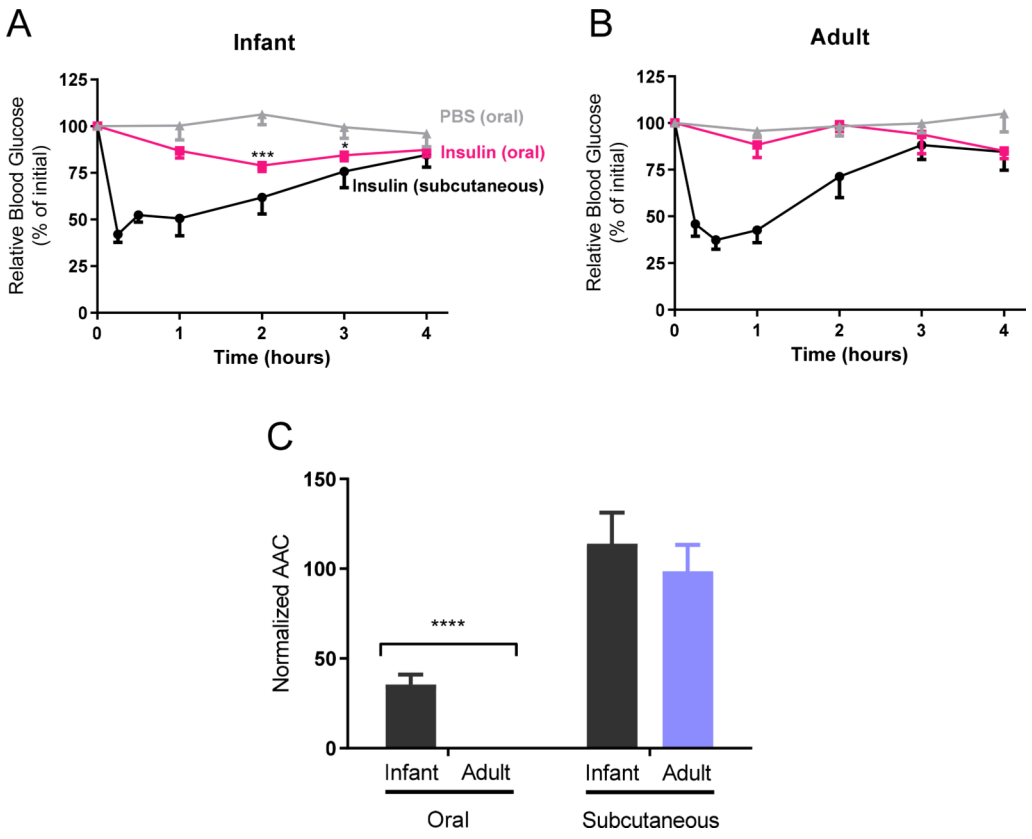

Fig. 5. –. Oral delivery of insulin lowers blood glucose levels in infant mice but not in adults.

A) Infant (2 week old) and B) adult (12 week old) mice were gavaged with either phosphate buffered saline (PBS) or 5 IU/kg insulin or subcutaneously injected with 1 IU/kg insulin. Blood glucose levels decreased after oral insulin in infant animals only. C) The oral normalized area above the curve (AAC) was significantly larger in infant animals. Blood glucose levels represent the mean ± SEM (n = 6). Two-way ANOVA with Bonferroni's multiple comparison; * $P < 0.05$, *** $P < 0.001$, compared to PBS (top panels). Student's unpaired *t* test: *** $P < 0.001$ compared to adult mice (bottom panel).

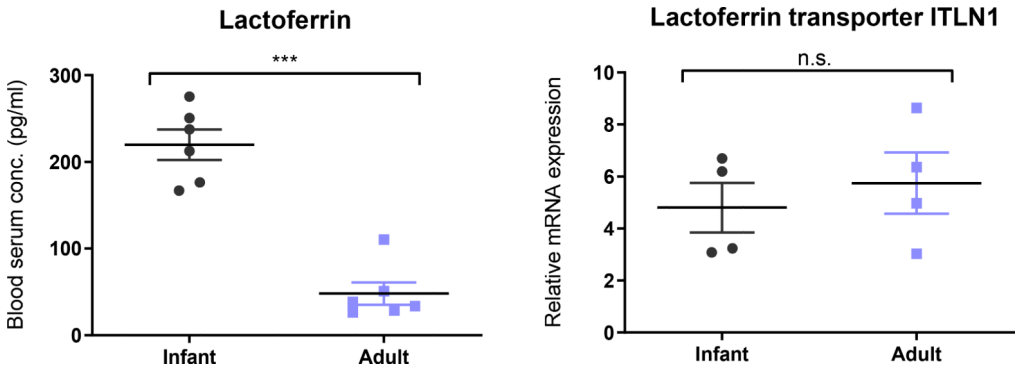

Fig 6 –. Oral absorption of lactoferrin is higher in infant mice due to increased paracellular permeability.

Animals were gavaged with human lactoferrin (320 mg/kg), and blood serum levels were measured by ELISA after two hours in infant (2 week old) and adult (12 week old) mice. Lactoferrin serum levels were significantly higher in infant mice, and mRNA expression of the lactoferrin transporter (ITLN1) was consistent across ages. Blood serum levels represent the mean ± SEM (n = 6). Student's unpaired *t* test: *** $P < 0.001$ compared to adult mice.

Table 1 –

Permeability of FITC-Dextrans decreased as a function of dextran size, mouse age, and intestinal tissue type. Apparent permeability (P_{app}; × 10^{-5} cm/s) of FITC-Dextran 4, 10, 70, and 150 kDa (FD). P_{app} values represent the mean ± SEM (n = 5).

	Proximal small intestine			Distal small intestine			Colon		
	2 wo	4 wo	12 wo	2 wo	4 wo	12 wo	2 wo	4 wo	12 wo
FD4	6.5 ± 0.9	3.1 ± 0.6	3.6 ± 0.4	4.4 ± 0.5	2.1 ± 0.3	1.6 ± 0.2	1.5 ± 0.3	1.1 ± 0.2	1.1 ± 0.2
FD10	3.8 ± 0.4	2.1 ± 0.3	1.8 ± 0.6	1.9 ± 0.3	1.0 ± 0.2	0.7 ± 0.1	0.5 ± 0.1	0.5 ± 0.1	0.5 ± 0.1
FD70	2.6 ± 0.3	1.2 ± 0.3	1.3 ± 0.2	2.1 ± 0.5	0.6 ± 0.4	0.3 ± 0.1	0.5 ± 0.1	0.3 ± 0.2	0.2 ± 0.1
FD150	0.9 ± 0.3	1.5 ± 0.1	1.1 ± 0.3	0.5 ± 0.2	0.2 ± 0.1	0.2 ± 0.1	0.2 ± 0.1	0.1 ± 0.1	0.2 ± 0.1

Table 2 -

mRNA expression of tight junctions in infant (2 week old) and adult (12 week old) mice intestines expressed as relative percentage of β actin.

Gene	Proximal small intestine		P value	Distal small intestine		P value	Colon		P value
	Infant	Adult		Infant	Adult		Infant	Adult	
CLDN1	0.016 ± 0.004	0.01 ± 0.002	0.251	0.009 ± 0.002	0.011 ± 0.003	0.53	0.029 ± 0.006	0.052 ± 0.017	0.208
CLDN2	**0.026 ± 0.007**	0.004 ± 0.002	0.004 **	0.034 ± 0.018	0.009 ± 0.003	0.145	0.036 ± 0.022	0.028 ± 0.007	0.725
CLDN3	0.546 ± 0.039	**0.987 ± 0.079**	0.0003 ***	0.312 ± 0.055	**1.346 ± 0.143**	0.0002 ***	0.874 ± 0.125	**5.042 ± 1.424**	0.021 *
CLDN4	**0.479 ± 0.099**	0.155 ± 0.013	0.0073 **	0.447 ± 0.041	0.259 ± 0.064	0.056	0.303 ± 0.036	0.44 ± 0.149	0.424
CLDN5	**0.091 ± 0.01**	0.018 ± 0.002	<0. 0001 ***	0.032 ± 0.004	0.035 ± 0.008	0.802	0.075 ± 0.019	0.122 ± 0.039	0.328
CLDN7	1.242 ± 0.053	**1.617 ± 0.102**	0.0115 *	0.856 ± 0.061	**1.831 ± 0.241**	0.009 **	1.024 ± 0.132	**4.252 ± 1.009**	0.008 **
CLDN8	0.202 ± 0.098	0.236 ± 0.082	0.795	**1.672 ± 0.301**	0.751 ± 0.241	0.036 *	1.633 ± 0.154	7.263 ± 3.373	0.153
CLDN12	0.021 ± 0.009	0.005 ± 0.001	0.113	0.012 ± 0.001	0.006 ± 0.002	0.354	0.072 ± 0.046	0.021 ± 0.003	0.327
CLDN13	0.038 ± 0.025	0.009 ± 0.002	0.209	0.016 ± 0.011	0.025 ± 0.008	0.509	0.035 ± 0.021	0.049 ± 0.016	0.613
CLDN15	0.543 ± 0.074	**1.164 ± 0.202**	0.013 *	0.169 ± 0.019	1.496 ± 0.591	0.109	0.243 ± 0.036	**1.775 ± 0.634**	0.05 *
ZO1	1.04 ± 0.101	**3.132 ± 0.414**	0.0003 ***	0.955 ± 0.086	**2.966 ± 0.301**	0.0004 ***	1.189 ± 0.142	**4.535 ± 0.232**	<0.0001 ***
ZO2	0.019 ± 0.008	0.029 ± 0.003	0.266	0.007 ± 0.001	0.064 ± 0.021	0.062	0.018 ± 0.002	0.07 ± 0.03	0.118
ZO3	0.072 ± 0.015	**0.376 ± 0.056**	0.0002 ***	0.044 ± 0.004	**0.469 ± 0.111**	0.013 *	0.048 ± 0.01	**0.421 ± 0.099**	0.004 **
OCLN	0.433 ± 0.063	**0.853 ± 0.127**	0.012 *	0.323 ± 0.032	**1.11 ± 0.23**	0.023 *	0.336 ± 0.049	**1.401 ± 0.41**	0.017 *
JAMA	0.846 ± 0.175	**1.868 ± 0.331**	0.018 *	0.68 ± 0.089	**1.984 ± 0.327**	0.008 **	0.835 ± 0.101	**2.154 ± 0.397**	0.005 **

Values that are significantly higher are in bold, n=6, Student's unpaired *t* test:

* $P < 0.05$

** $P < 0.01$

*** $P < 0.001$.